

AD-A184 267

EFFECTS OF CURE PRESSURE ON RESIN FLOW VOIDS AND
MECHANICAL PROPERTIES. (U) STANFORD UNIV CA DEPT OF
AERONAUTICS AND ASTRONAUTICS G S SPRINGER ET AL.

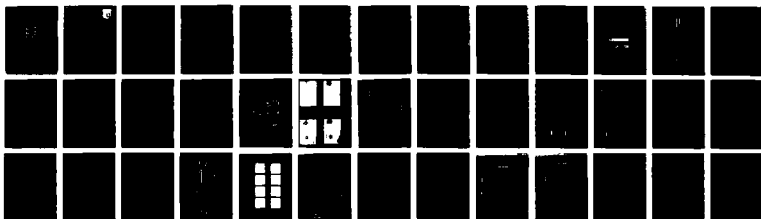
1/1

UNCLASSIFIED

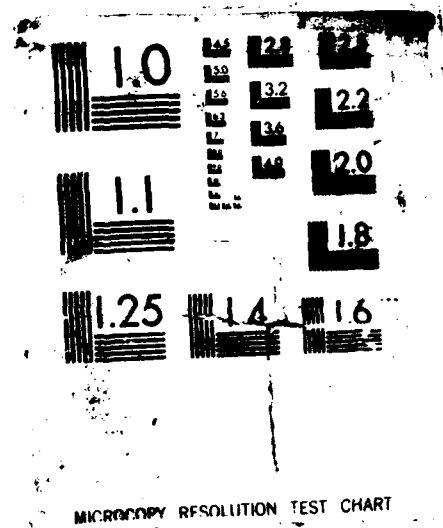
JUL 87 AFMRL-TR-87-4858 F33615-84-C-5849

F/G 11/4

NL



END
9-87
DTIC



MICROCOPY RESOLUTION TEST CHART

AFWAL-TR-87-4058



**EFFECTS OF CURE PRESSURE ON RESIN FLOW, VOIDS,
AND MECHANICAL PROPERTIES**

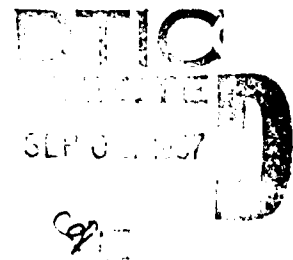
George S. Springer, Jian-Mao Tang, and Woo I. Lee
Department of Aeronautics and Astronautics
Stanford University, Stanford, California

July 1987

Interim Report for Period May 1986--April 1987

Approved for public release; distribution unlimited.

MATERIALS LABORATORY
AIR FORCE WRIGHT AERONAUTICAL LABORATORIES
AIR FORCE SYSTEMS COMMAND
WRIGHT-PATTERSON AIR FORCE BASE, OHIO 45433-6533



87 1 101
87 9 1 101

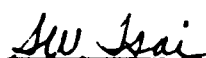
NOTICE

When government drawings, specifications, or other data are used for any purpose other than in connection with a definitely related Government-related procurement, the United States government incurs no responsibility or any obligation whatsoever. The fact that the Government may have formulated or in any way supplied the said drawings, specifications, or other data, is not to be regarded by implication or otherwise as in any manner construed, as licensing the holder, or any other person or corporation; or as conveying any rights or permission to manufacture, use, or sell any patented invention that may in any way be related thereto.

This report has been reviewed by the Office of Public Affairs (ASD/PA) and is releasable to the National Technical Information Service (NTIS). At NTIS, it will be available to the general public, including foreign nations.

This technical report has been reviewed and is approved for publication.

FOR THE COMMANDER



STEPHEN W. TSAI, Chief
Mechanics & Surface Interactions Br
Nonmetallic Materials Division



MERRILL L. MINGES, SES, Director
Nonmetallic Materials Division

If your address has changed, if you wish to be removed from our mailing list, or if the addressee is no longer employed by your organization, please notify **AFWAL/MLBM**, Wright-Patterson AFB, OH 45433-6533 to help us maintain a current mailing list.

Copies of this report should not be returned unless return is required by security considerations, contractual obligations, or notice on a specific document.

6a NAME OF PERFORMING ORGANIZATION Stanford University		6b OFFICE SYMBOL (If applicable)		7a NAME OF MONITORING ORGANIZATION Materials Laboratory (AFWAL/MLBM) Air Force Wright Aeronautical Laboratories	
6c ADDRESS (City, State, and ZIP Code) Stanford, CA 94305				7b ADDRESS (City, State, and ZIP Code) Wright-Patterson AFB, OH 45433-6533	
8a NAME OF FUNDING/SPONSORING ORGANIZATION		8b OFFICE SYMBOL (If applicable)		9 PROCUREMENT INSTRUMENT IDENTIFICATION NUMBER F33615-84-C-5049	
8c ADDRESS (City, State, and ZIP Code)				10 SOURCE OF FUNDING NUMBERS	
PROGRAM ELEMENT NO 62102F		PROJECT NO 2419		TASK NO 01	WORK UNIT ACCESSION NO 67
11 TITLE (Include Security Classification) Effects of Cure Pressure on Resin Flow, Voids, and Mechanical Properties					
12 PERSONAL AUTHOR(S) Jian-Mao Tang, Woo I. Lee, and George S. Springer					
13a TYPE OF REPORT Interim		13b TIME COVERED FROM 5/86 TO 4/87		14 DATE OF REPORT (Year, Month, Day) 1987, July	
15 PAGE COUNT 43					
16 SUPPLEMENTARY NOTATION					
17 COSATI CODES			18 SUBJECT TERMS (Continue on reverse if necessary and identify by block number)		
FIELD	GROUP	SUB-GROUP	composite materials, cure, cure pressure		
11	04				
19 ABSTRACT (Continue on reverse if necessary and identify by block number) <p>The effects of cure pressure on resin flow, compaction, void content, and mechanical properties of fiber reinforced composites were investigated. Tests were performed on laminates made of Fiberite T300/976 and T300/934 unidirectional prepreg tape. Data are presented on compaction, resin flow, and void content which tend support to the validity of the Springer-Loos model. Data are also given showing the effects of cure pressure on void content and on the compressive strength and short-beam shear strength and modulus.</p>					

FOREWORD

This work was performed in the Department of Aeronautics and Astronautics, Stanford University, under the support of the Mechanics and Surface Interactions Branch (AFWAL/MLBM), Nonmetallic Materials Division, Materials Laboratory, Air Force Wright Aeronautical Laboratories, Wright-Patterson Air Force Base, Ohio; Project Number 2419, "Non-metallic Structural Materials," Task Number 241901, "Composite Materials and Mechanics Technology," Contract Number F33615-84-C-5049.

Accession For	
ADIS GRA&I	<input checked="" type="checkbox"/>
DTIC TAB	<input type="checkbox"/>
Unannounced	<input type="checkbox"/>
Justification	
By _____	
Distribution/	
Availability Codes	
Avail and/or	
Dist	Special
A-1	



TABLE OF CONTENTS

Section	Page
I INTRODUCTION	1
II DESCRIPTION OF RESIN FLOW AND PRESSURE DISTRIBUTION	2
Resin Flow	2
Pressure Distribution	5
III EXPERIMENTAL VERIFICATION	10
Compaction	10
Pressure Distribution and Resin Flow	14
Void Content	23
IV MECHANICAL PROPERTIES	27
V CONCLUDING REMARKS	31
REFERENCES	32
APPENDIX A. Number of Compacted Plies	33
APPENDIX B. Resin Flow in Fiberite T300/934 Laminates	35

LIST OF FIGURES

Figure		Page
1	Illustration of possible resin flow patterns. Resin may originate from the space between the fibers (dotted lines) and from the space between adjacent plies (solid lines).	3
2	Illustration of possible resin flow patterns a) resin flow only normal to the plies, b) resin flow only parallel to the plies, c) resin flow normal and parallel to the plies. Flow pattern depends on geometry (width to thickness ratio), edge constraints ("dams") and bleeder arrangements.	4
3	Illustration of the resin flow and compaction processes a) resin flow only normal to the plies, b) resin flow only parallel to the plies, c) resin flow normal and parallel to the plies.	6
4	Pressure distribution inside the laminate (right) and the linear pressure distribution assumed in the Loos-Springer model (left).	7
5	Fiber volumes at which load carried by the fibers is or is not significant. Data from Ref. [6].	8
6	Schematic of the apparatus used for studying the compaction of rods immersed in a viscous liquid [9].	11
7	Photographs showing the compaction of rods immersed in a liquid [9].	12
8	The thickness of each ply at the end of the cure of 60 ply AS/3501-6 laminates. Data extracted from the photomicrographs of Campbell [4]. n_c is the number of compacted plies.	13
9	Resin flow (mass loss) in unidirectional composites parallel to the plies and normal to the plies. Data from Ref. [2]. Comparisons between the data and the results computed by the Loos-Springer model [2].	16
10	Resin flow (mass loss) in cross-ply composites parallel to the plies and normal to the plies. Data from Ref. [10]. Comparisons between the data and the results computed by the Loos-Springer model [2].	17
11	The cure cycle used in preparing Fiberite T300/976 and T300/934 laminates.	18
12	Resin flow in Fiberite T300/976 unidirectional composites normal to the plies at the end of the cure. Comparisons between the data and the results computed by the Loos-Springer model [2]. Cure cycle given in Figure 11.	19
13	Resin content in the bleeder for Fiberite T300/976 unidirectional	20

composites at the end of the cure. Comparisons between the data and the results computed by the Loos-Springer model [2]. Cure cycle given in Figure 11.

14	Illustration of the effect of bleeder thickness. If the bleeder is too thin (left), the bleeder becomes saturated before compaction is complete and resin rich layers are present. For thick bleeder (right), all the resin is squeezed out at the end of the cure.	24
15	Photomicrographs of eight-ply Fiberite T300/976 and T300/934 laminates cured at 0 (vacuum bag), 20, 55, and 80 psig pressure. Magnification is 100 times. Temperature cure cycle is shown in Figure 11.	25
16	Void contents as a function of cure pressure of Fiberite T300/976 and T300/934 eight-ply unidirectional laminates. Circles are data deduced from the photomicrographs of Figure 15. Bars represent spread in the data. Solid line is the result computed by the Loos-Springer model [2].	26
17	Geometries of the compression and short-beam shear specimens.	28
18	The longitudinal compressive strengths of Fiberite T300/976 (16-ply) and T300/934 (20-ply) unidirectional laminates as a function of void content and cure pressure. Bars represent spread in the data. Cure cycle given in Figure 11.	29
19	The short-beam shear strengths and moduli of Fiberite T300/976 (16-ply) and T300/934 (20-ply) unidirectional laminates as a function of void content and cure pressure. Bars represent spread in the data. Cure cycle given in Figure 11.	30
B-1	Resin flow in Fiberite T300/934 (20-ply) unidirectional composites normal to the plies as a function of cure pressure (left) and bleeder thickness (right) at the end of cure. Cure cycle given in Figure 11.	36

Section I

INTRODUCTION

Curing of thermoset resin composites requires the application of heat and pressure. Heat is used to facilitate and control the chemical reactions. Pressure is applied to squeeze out excess resin, to consolidate plies, and to minimize void content. Thus, to ensure proper cure, the magnitudes and durations of the heat and pressure (referred to as the "cure cycle") must be chosen carefully.

The cure cycle can be established either empirically or by the use of models. Empirical methods require large number of tests with different heating rates and pressures. Such empirical, "trial and error" procedures are expensive and time consuming, and are restricted to small ranges of process variables.

Models which simulate the cure process provide a convenient means of establishing the proper cure cycle. A model suitable for simulating the curing of thermoset resin composites has been developed previously (e.g., see Refs. 1 and 2). This model is composed of submodels among which are the "thermo-chemical" sub-model (giving the temperature, viscosity, and degree of cure), the "flow" submodel (yielding the pressure distribution, resin flow, and compaction) and the "void" submodel (resulting in the void sizes). The thermo-chemical submodel has been verified by numerous tests [2-4] and its validity generally is unquestioned. Fewer data are available pertaining to the flow and void submodels, and some of these data are contradictory, having given rise to misunderstandings regarding the pressure. Therefore, the objective of this investigation was to examine the role of pressure in the curing process, and to evaluate the effects of pressure on resin flow, compaction, void content, and mechanical properties.

Section II

DESCRIPTION OF RESIN FLOW AND PRESSURE DISTRIBUTION

In order to assess the role of pressure in the cure process, the pressure distribution inside the composite must be known. In the following qualitative descriptions of the pressure distribution and resin flow are given. Pertinent experimental data are presented in the next section.

The discussion will address the resin flow and pressure distributions in laminates consisting of layers (plies) of unidirectional "prepreg" tape. The same reasoning and conclusions apply to composites made of layers of woven fabrics when resin flow is primarily in the direction perpendicular to the laminate.

Resin Flow

Upon application of pressure resin may be "squeezed out" from the spaces between the individual fibers and from the space between adjacent plies (Figure 1). In fact, owing to the proximity of the fibers, relatively small amount of resin is removed from the space between the fibers. The bulk of the resin originates from the space between adjacent plies. Depending on the width to thickness ratio, edge constraints, and bleeder arrangements, resin may flow in the direction normal to the plane of the laminate (Figure 2a), parallel to the laminate (Figure 2b) or both normal and parallel to the laminate (Figure 2c).

The motion and rearrangement of the plies due to the resin flow is illustrated in Figure 3. When the resin flow is only in the normal direction then first only the top layer moves, while resin is being squeezed out from space between the first and second layers (Figure 3a). When the fibers reach the second layer, the first two layers move in unison towards the third layer, squeezing resin out from the space between the second and third layers. This sequence is repeated for the subsequent layers. Thus, the layers are "compacted" in a wavelike, cascading manner. When resin flow is only in the direction parallel to the plies,

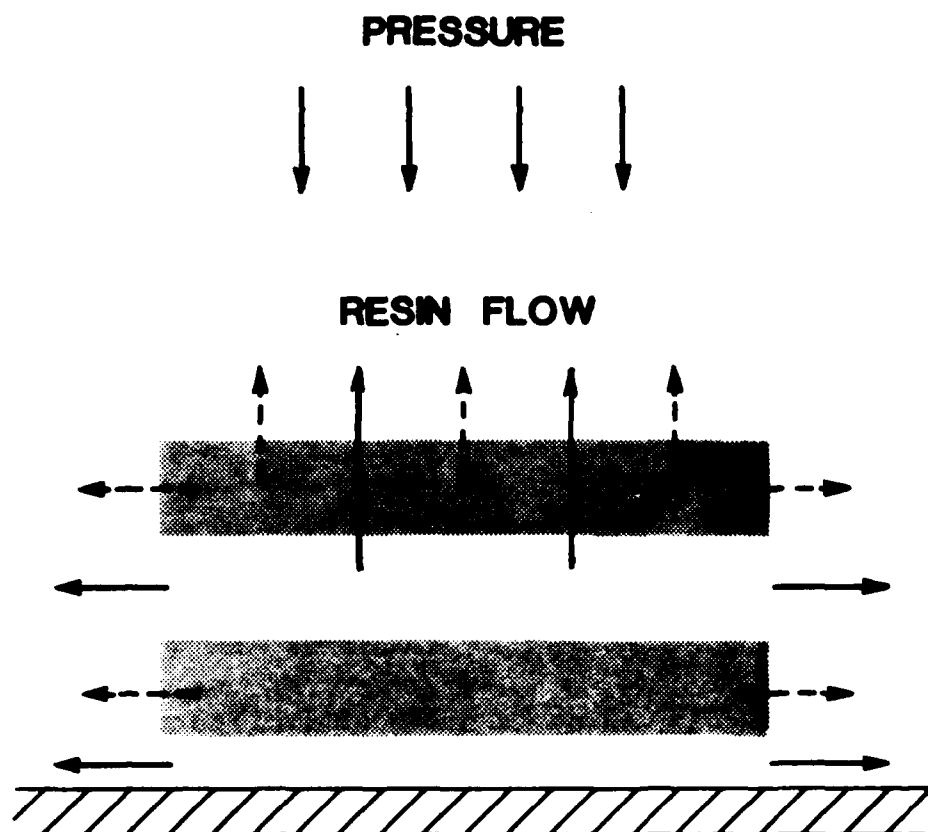


Fig. 1. Illustration of possible resin flow patterns. Resin may originate from the space between the fibers (dotted lines) and from the space between adjacent plies (solid lines).

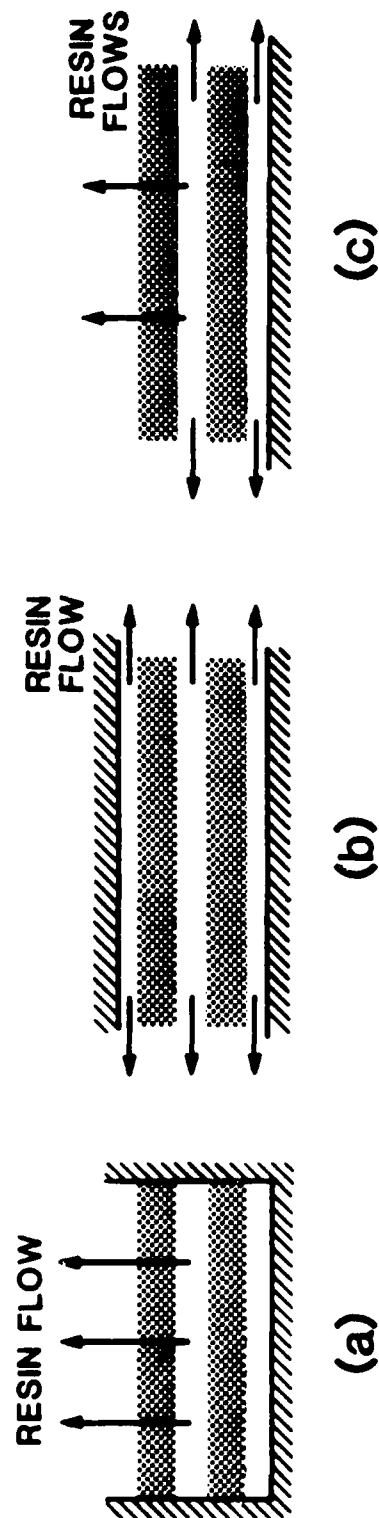


Fig. 2. Illustration of possible resin flow patterns a) resin flow only normal to the plies, b) resin flow only parallel to the plies, c) resin flow normal and parallel to the plies. Flow pattern depends on geometry (width to thickness ratio), edge constraints ("dams") and bleeder arrangements.

the plies compact nearly uniformly (Figure 3b). When resin flow is both in the normal and parallel directions, the plies compact in the manner illustrated in Figure 3c.

Pressure Distribution

The pressure distribution inside the laminate is dictated by the physics of the problem. A pressure differential exists only across regions where resin flow occurs. In the absence of resin flow there is no pressure drop and, consequently, in the "no flow" regions the pressure is constant. These considerations require the pressure distributions to be as follows.

When resin flows only in the direction normal to the plies there is a pressure drop across the compacted plies and inside the bleeder as shown in Figure 4. When there is resin flow in the direction parallel to the plies, there is a pressure drop along the laminate from the center of the laminate to the edge (Figure 4). A force balance requires that the pressure at the center of the plate be equal to or *higher* than the applied pressure (Figure 4).

Recently, there have been some data reported which suggest that, as the cure progresses, the pressure in the resin at the bottom center of the laminate becomes lower than the applied pressure [4-5]. Such decrease in resin pressure could occur only if the fibers were to "touch" and hence carry load. This situation does not arise as long as all the fibers are surrounded by resin, i.e., until there is at least one thin resin layer in the prepreg across which there is no fiber-to-fiber contact (Figure 5). Thus, (when resin flow is only in the direction normal to the plies) pressure drop occurs across the compacted plies only, and (until full compaction occurs) the pressure on the bottom of the prepreg is the same as the applied pressure

$$P^* = \frac{P_{\text{bottom}}}{P_{\text{applied}}} = 1 \quad (\text{no load carried by fibers}) \quad (1)$$

Only when there is fiber contact do fibers carry some of the load. In this case there is a pressure drop across the thickness of the prepreg

$$P^* = \frac{P_{\text{bottom}}}{P_{\text{applied}}} < 1 \quad (\text{load carried by fibers}) \quad (2)$$

Recent tests by Gutowski et al. have shown that the load carried by the fibers (and correspondingly the resin pressure drop) becomes appreciable only at fiber volume fractions

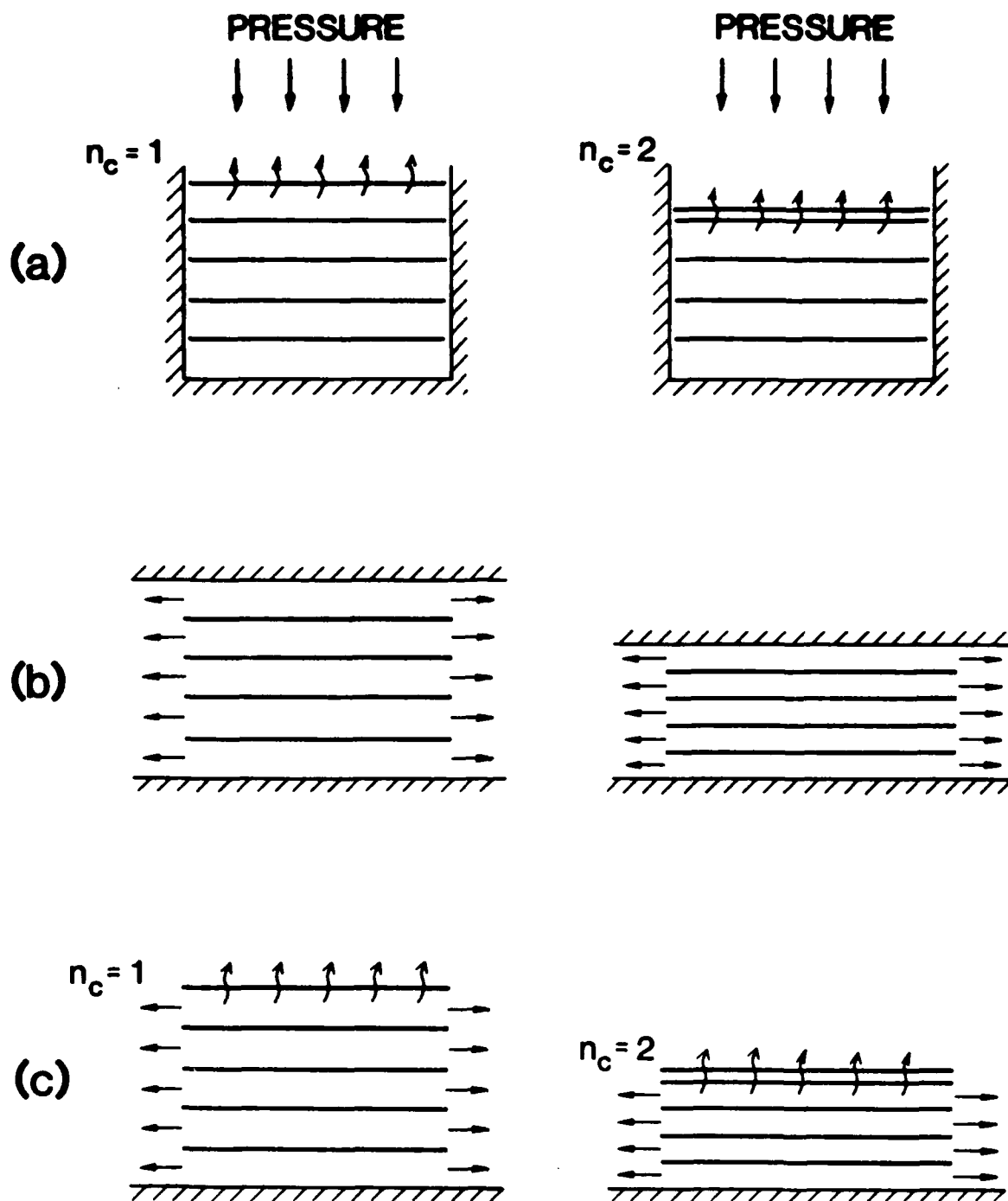


Fig. 3. Illustration of the resin flow and compaction processes a) resin flow only normal to the plies, b) resin flow only parallel to the plies, c) resin flow normal and parallel to the plies.

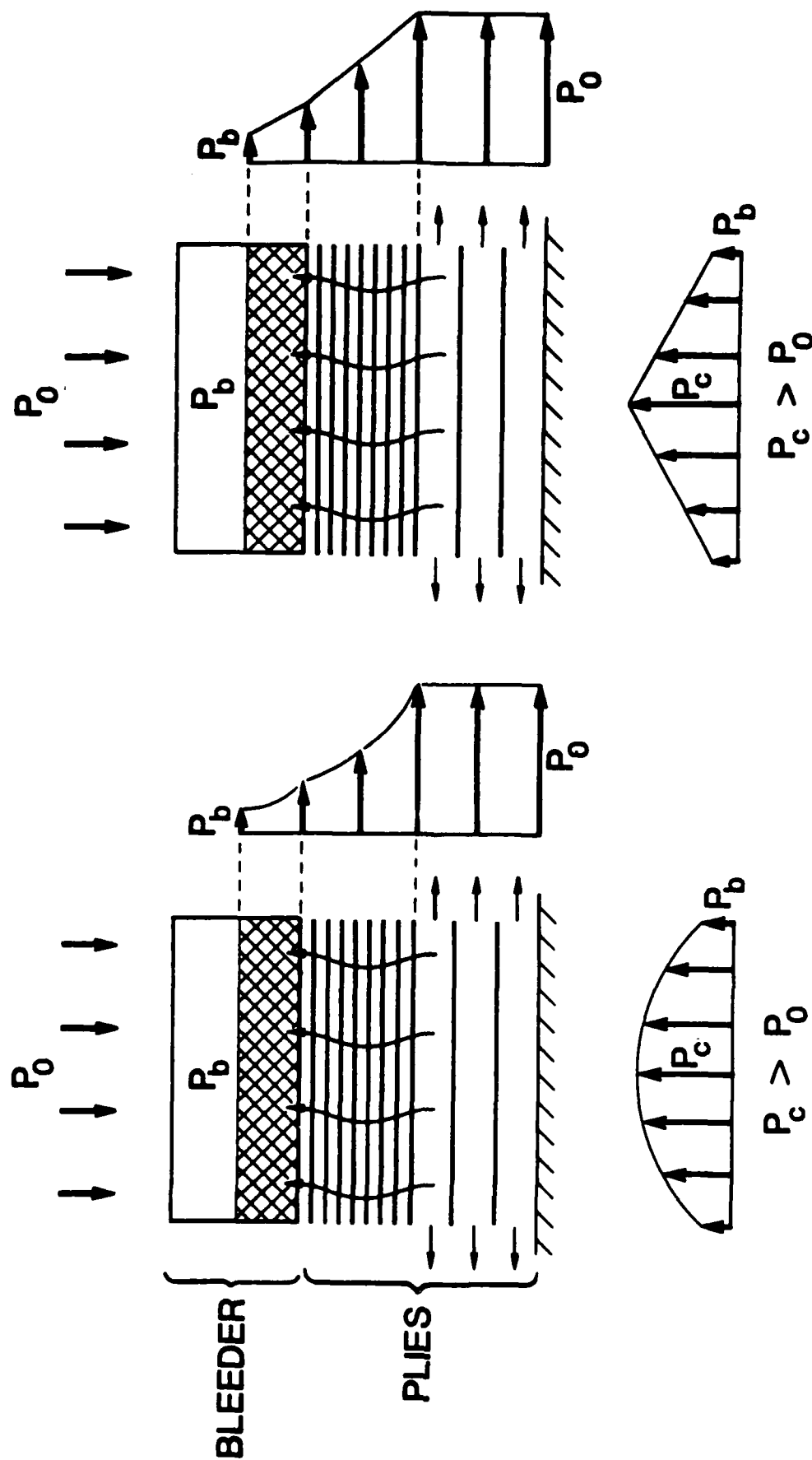


Fig. 4. Pressure distribution inside the laminate (right) and the linear pressure distribution assumed in the Loose-spring model (left).

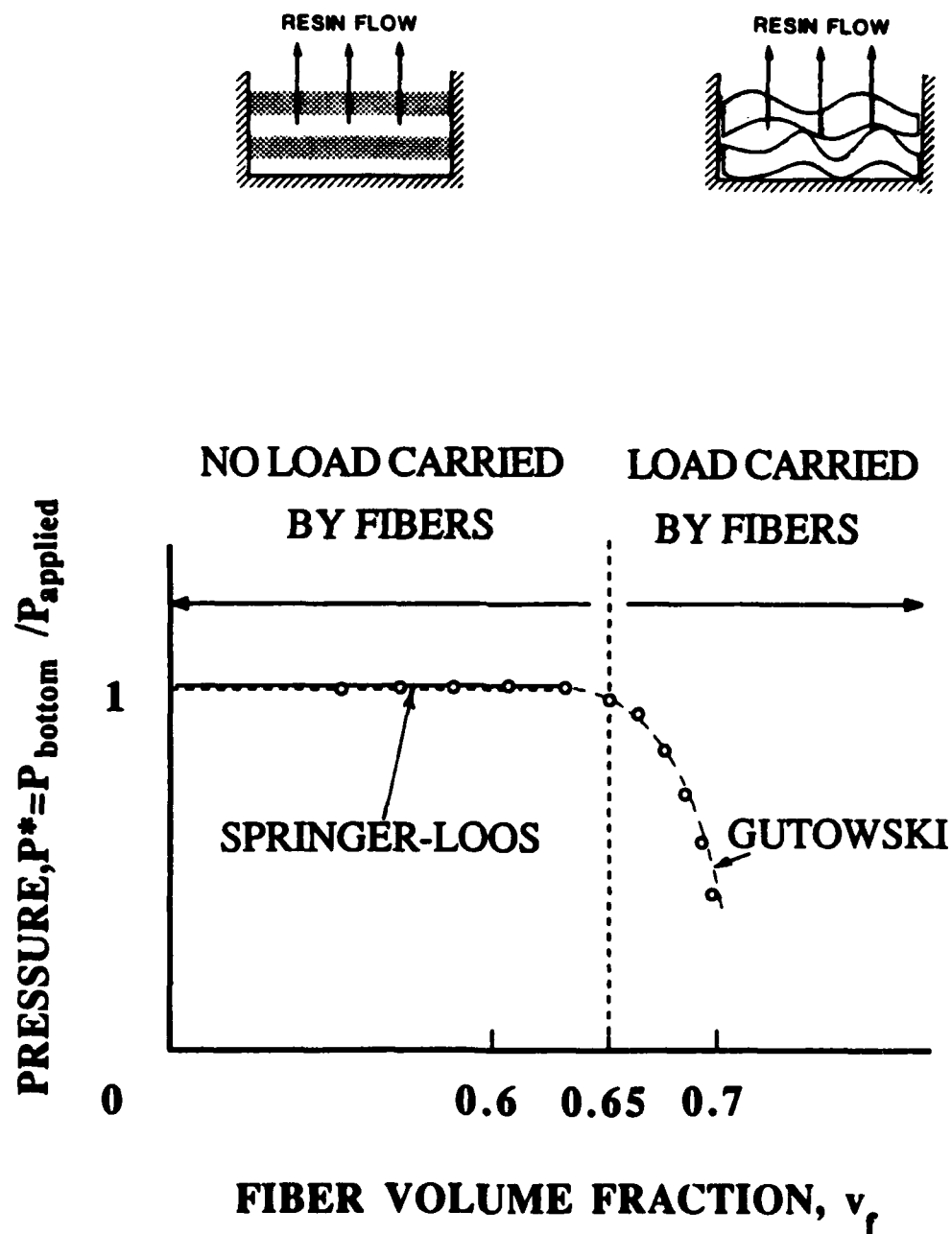


Fig. 5. Fiber volumes at which load carried by the fibers is or is not significant. Data from Ref. [6].

above 0.6 to 0.7 percent [6]. This situation was taken into account in a model proposed by Gutowski [7, 8]. It is worth noting that at fiber volume fractions below 0.6 to 0.7 percent the Springer-Loos and Gutowski models provide nearly the same results.

Section III

EXPERIMENTAL VERIFICATION

The general descriptions of resin flow and pressure distribution presented in the previous section can be confirmed by experimental data. Some of the phenomenon, such as compaction can be observed directly. Some of the data can be interpreted with the use of models. A model simulating the cure process was described by Loos and Springer [1, 2]. Details of this model are not given here. Essentially, for specified material, geometry, cure temperature and cure pressure, the model yields the following information: a) resin flow normal and parallel to the plane of the plies, b) resin content of the bleeder, c) compaction, and d) changes in void diameters.

Compaction

The compaction process has been demonstrated both with "model" systems and with actual laminates made of prepreg tape. Compaction in a model system was demonstrated by Springer [9], who studied the motion of rods suspended in a viscous fluid. Springer's apparatus and photographs showing the compaction process are reproduced here in Figures 6 and 7. These photographs demonstrate clearly the wavelike nature of the compaction.

The compaction process was also demonstrated for thick graphite-epoxy laminates by Campbell et al. [4] who took photomicrographs of composites cured at different pressures. The thickness of each ply was determined from Campbell's photomicrographs. (In Figure 40 of Ref. 4, the tool plate appears to be on the top of the photograph for 100 psig cure pressure and on the bottom for the other cure pressures.) The results are plotted in Figure 8. As can be seen, the data follows the expected trend. Only the plies nearest to the bleeder compacted. The plies at the bottom (next to the tool plate) did not compact. Furthermore, the number of compacted plies increased with increasing pressure, as required by the physics of the problem described in the previous section.

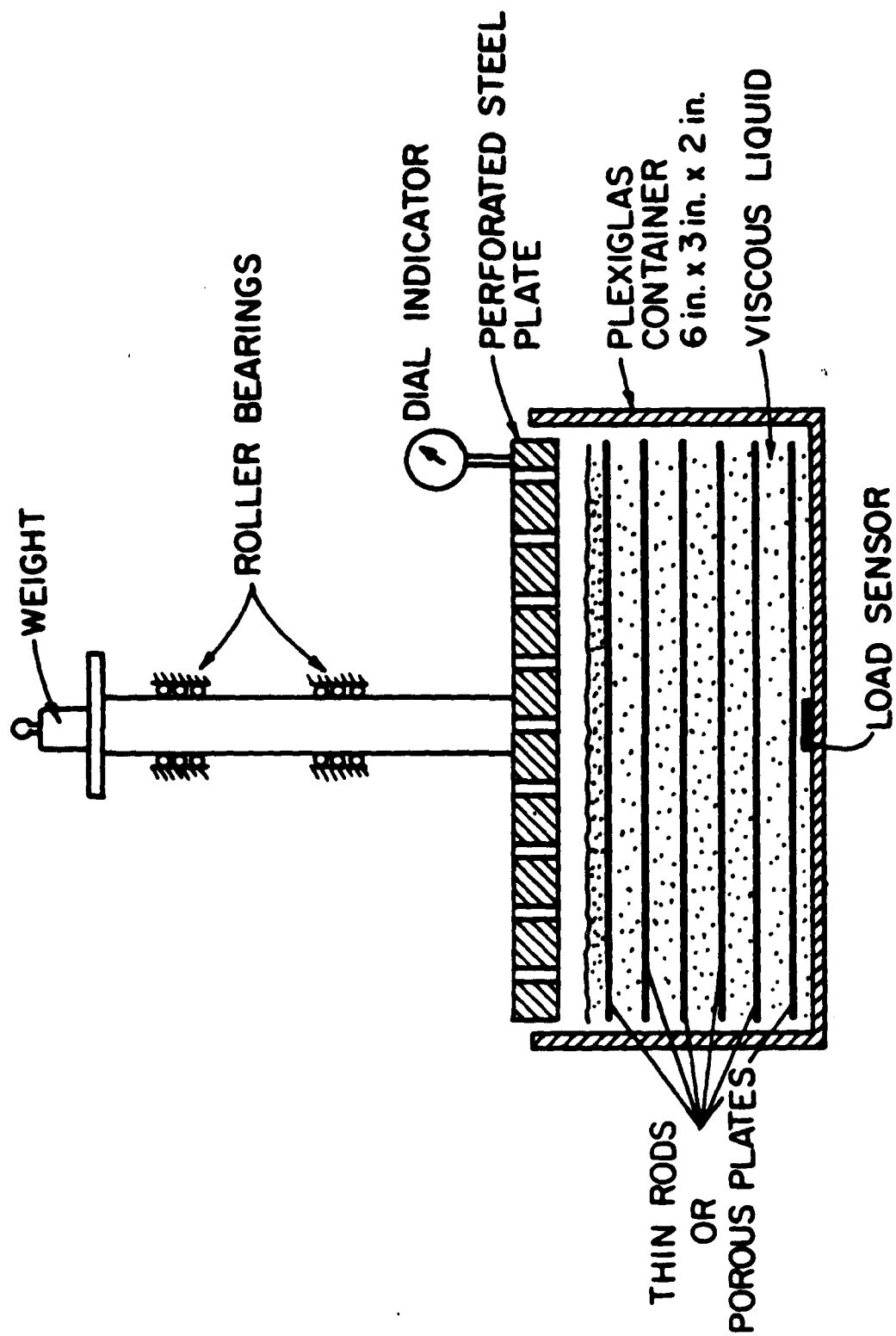
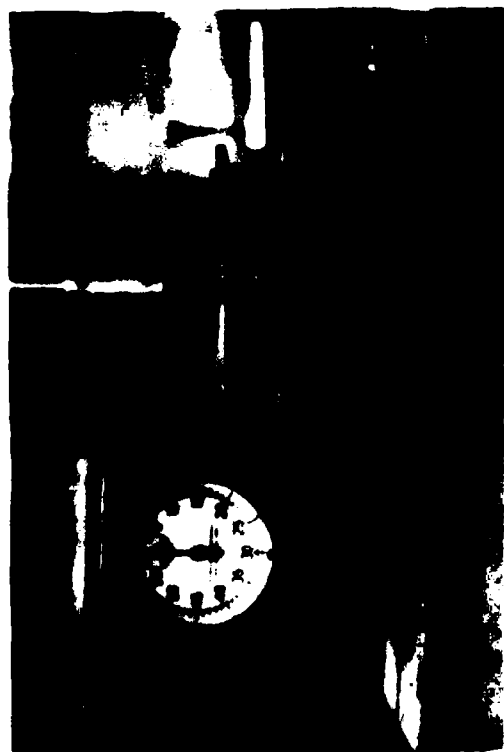
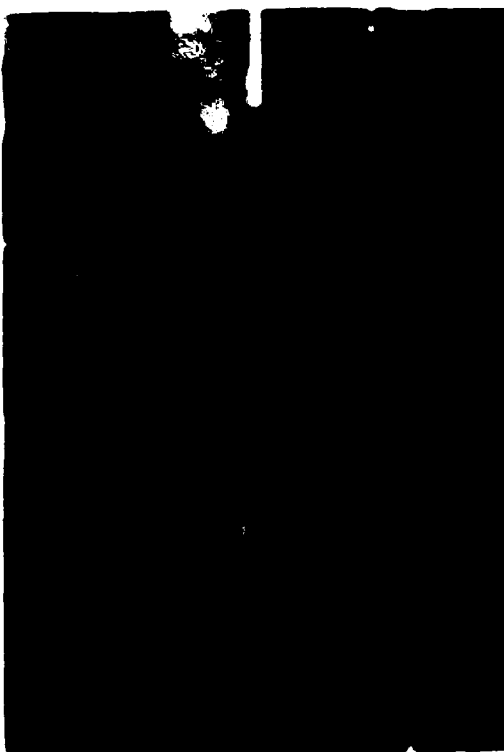


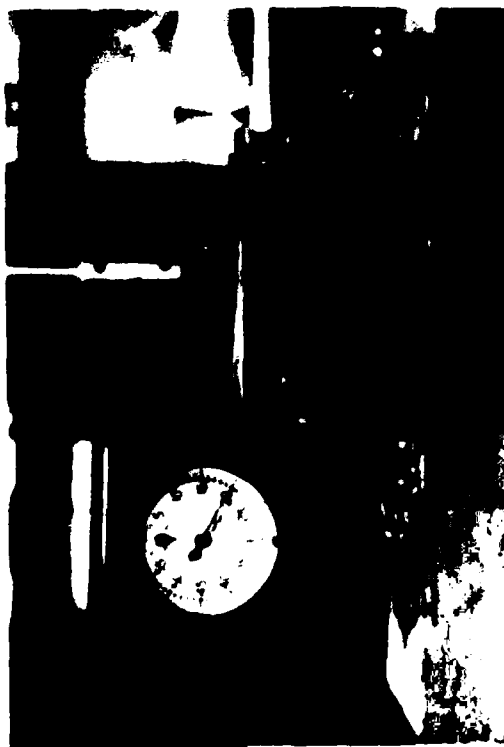
Fig. 6. Schematic of the apparatus used for studying the compaction of rods immersed in a viscous liquid [9].



$t = 0 \text{ sec}$



$t = 210 \text{ sec}$



$t = 80 \text{ sec}$



$t = 360 \text{ sec}$

Fig. 7. Photographs showing the compaction of rods immersed in a liquid [9].

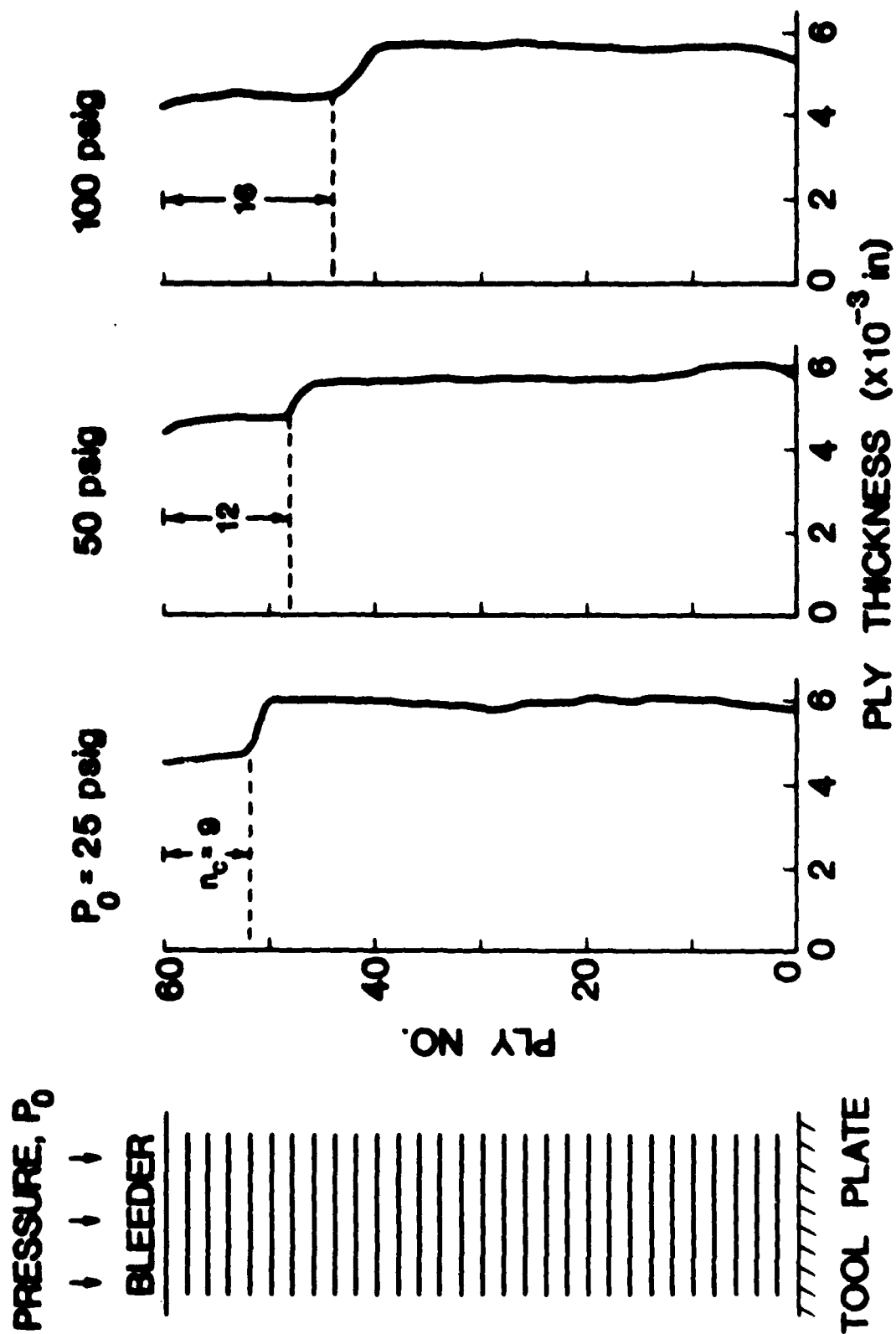


Fig. 8. The thickness of each ply at the end of the cure of 60 ply AS/3501-6 laminates. Data extracted from the photomicrographs of Cam' is the number of compacted plies.

Provided that the model and the presumed pressure distribution inside the resin are correct, the number of compacted plies n_c can be estimated by the expression (see Appendix A)

$$n_c = C\sqrt{P_o - P_b} \quad (3)$$

where P_o is the applied (cure) pressure and P_b is the pressure in the bleeder. C is a constant which depends on the geometry and the material properties.

For a cure pressure of $P_o = 25$ psig and bleeder pressure of P_b , the data in Figure 8 show that the number of compacted plies is $n_c = 9$. For these values of P_o , P_b , and n_c the constant C becomes $C = 1.47 (\text{psi})^{-\frac{1}{2}}$. With this value of C the calculated number of compacted plies is 11.6 and 15.6 for 50 psig and 100 psig cure pressures, respectively. These calculated values compare favorably with the number of plies actually compacted (see Figure 8 and Table 1), providing additional evidence of the validity of the model.

Pressure Distribution and Resin Flow

Measured resin flows were compared to resin flows computed by the Loos-Springer model to assess the validities of the model and the assumed pressure distributions.

Resin flows in unidirectional and cross-ply AS/3501-6 laminates were measured by Loos and Springer [2] and by Loos and Freeman [10]. Their data are reproduced in Figures 9 and 10. Resin flows in laminates made of Fiberite T300/976 unidirectional prepreg tape were measured in the present investigation. The results are shown in Figures 12 and 13, and give a) the resin flow normal to the plane of the plies as a function of pressure and b) the resin content inside the bleeder.

The resin flow data given in Figures 9 through 13 were compared with the results of the Loos-Springer model. The material properties used in the calculations are given in Tables 2 and 3. The comparisons between the data and the results of the model are included in Figures 9, 10, 12, and 13. The model predicts quite accurately the resin flow, indicating that the pressure distribution assumed in the calculations are adequate for calculating the resin flow.

TABLE 1

Number of compacted plies taken from Campbell's Tests (Figure 8)
and computed by the Loos-Springer Model (Eq. 1)

Laminate: AS/3501-6 60-ply

Cure Pressure, P_0 (psig)	Number of Compacted Plies	
	Measured	Calculated
25	8	9
50	12	11
25	16	15

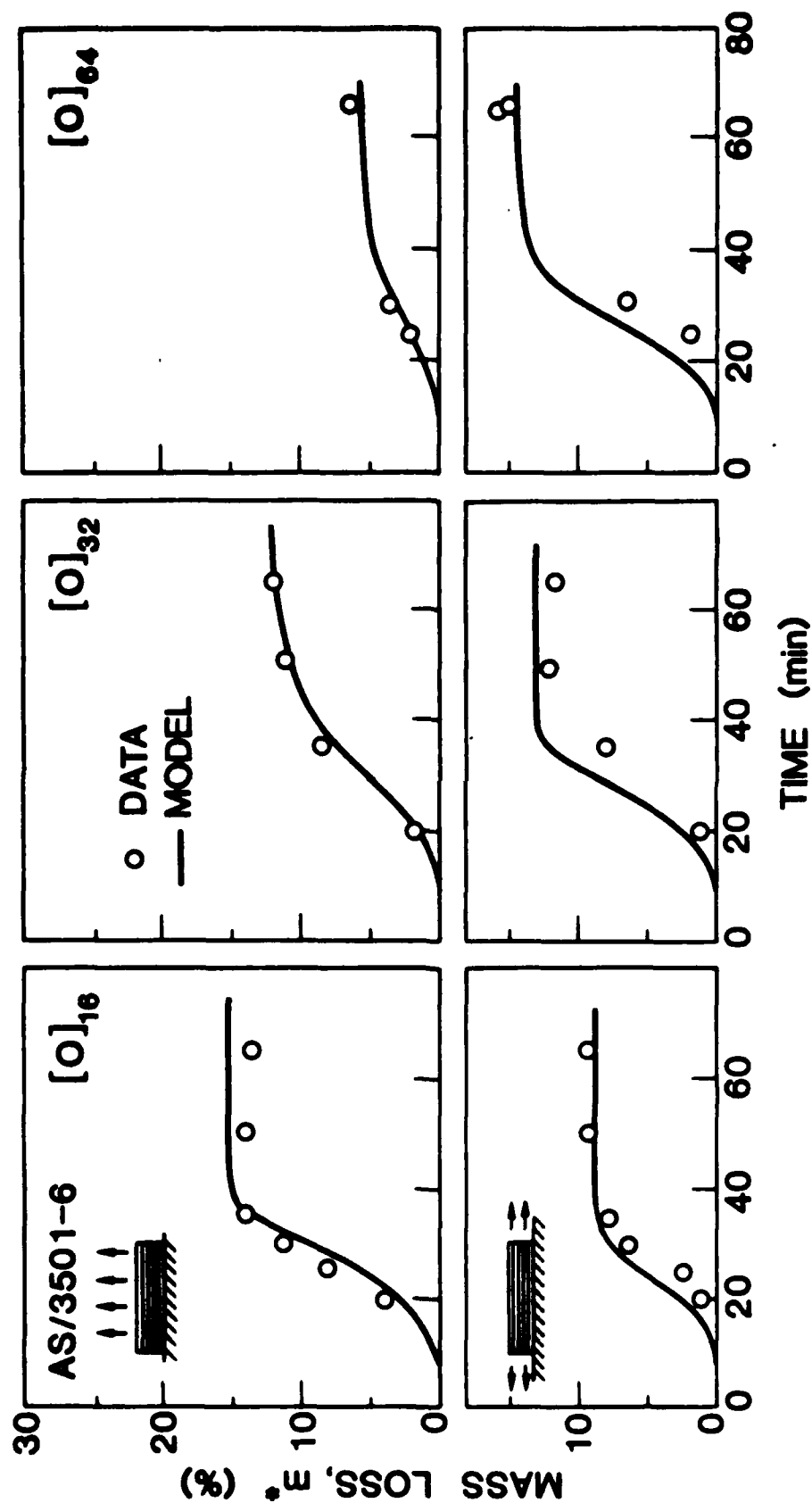


Fig. 9. Resin flow (mass loss) in unidirectional composites parallel to the plies and normal to the plies. Data from Ref.[2]. Comparisons between the data and the results computed by the Loss-Springer model [2].

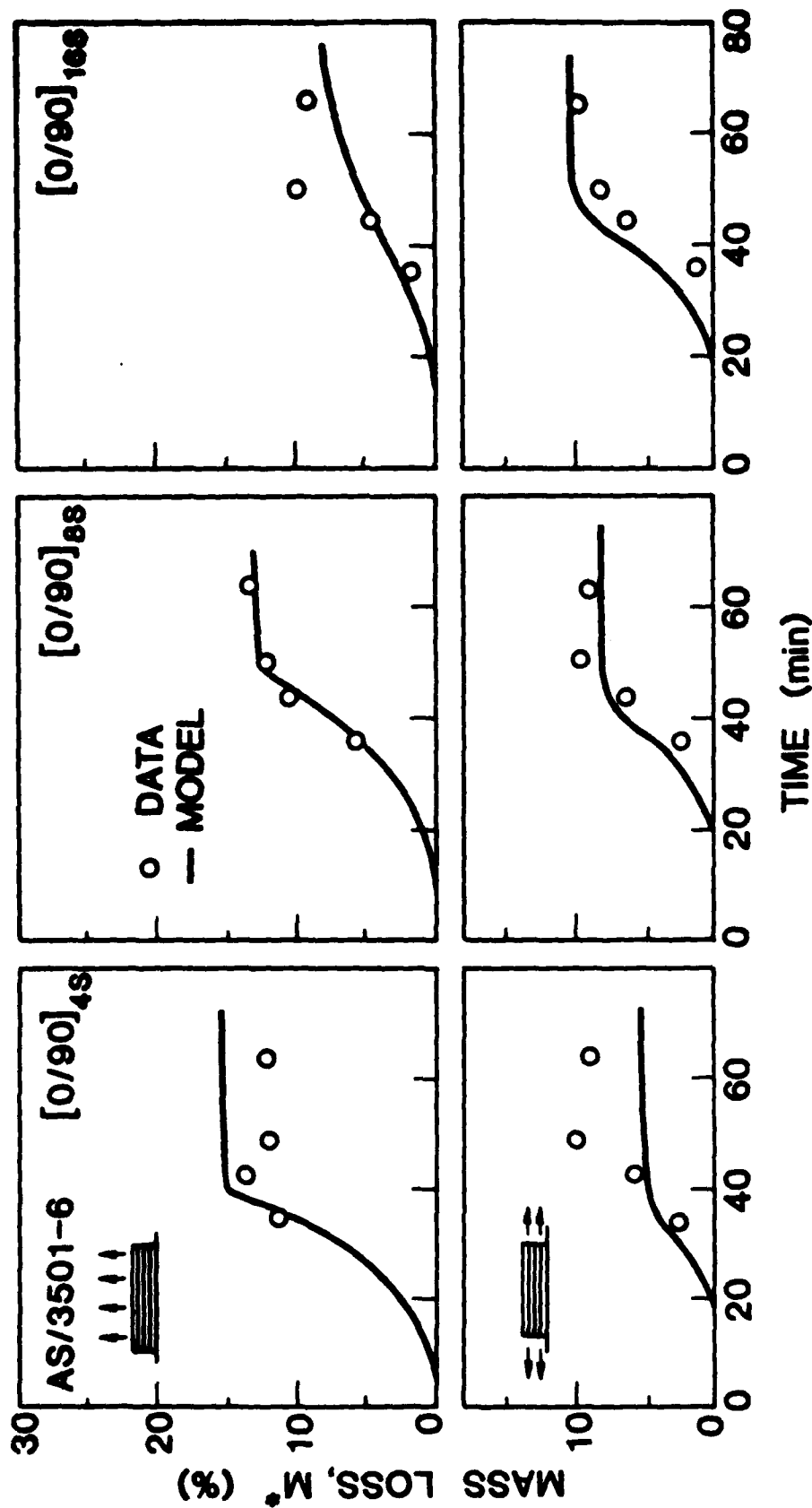


Fig. 10. Resin flow (mass loss) in cross-ply composites parallel to the plies and normal to the plies. Data from Ref. [10]. Comparisons between the data and the results computed by the Loos-Springer model [2].

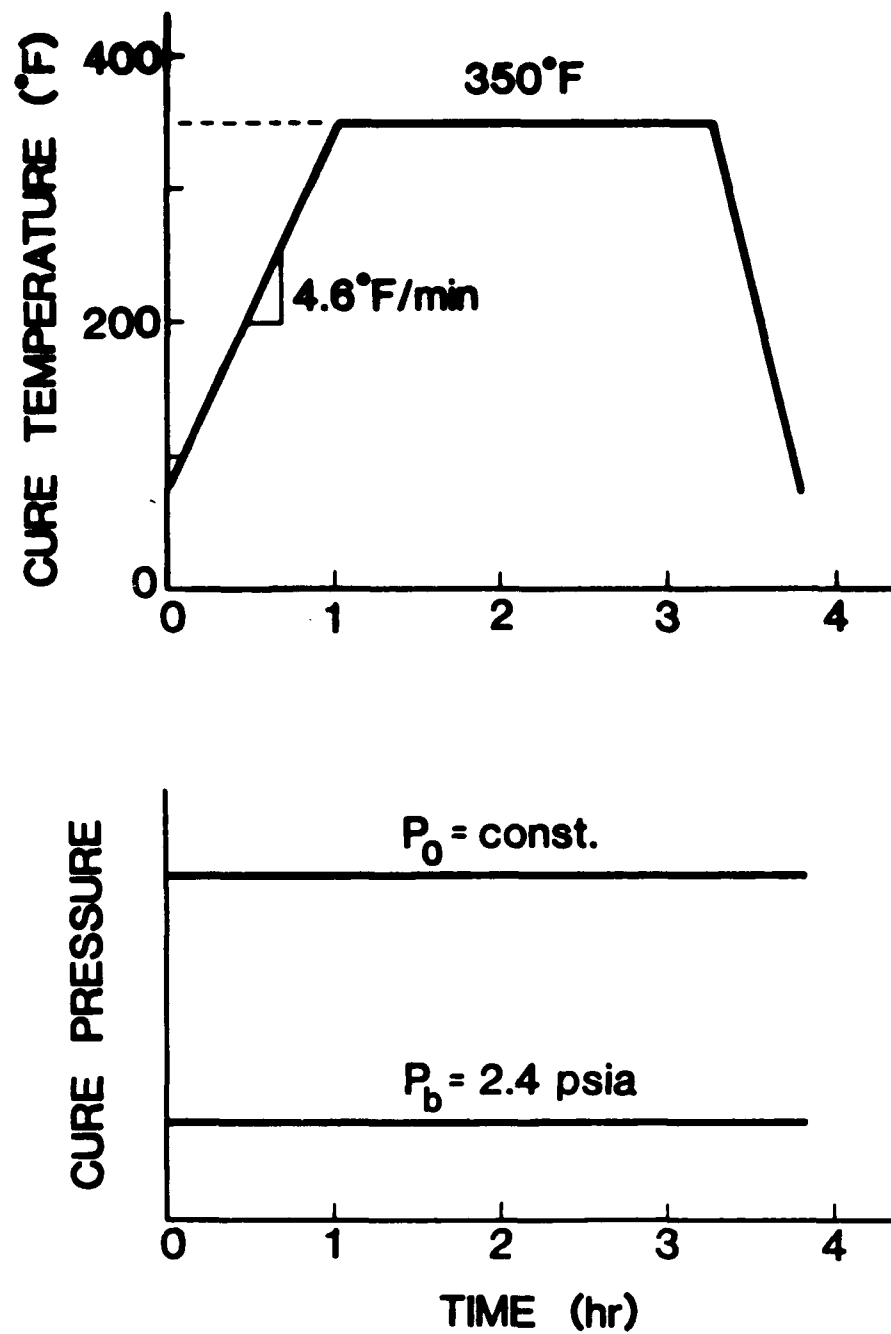


Fig. 11. The cure cycle used in preparing Fiberite T300/976 and T300/934 laminates.

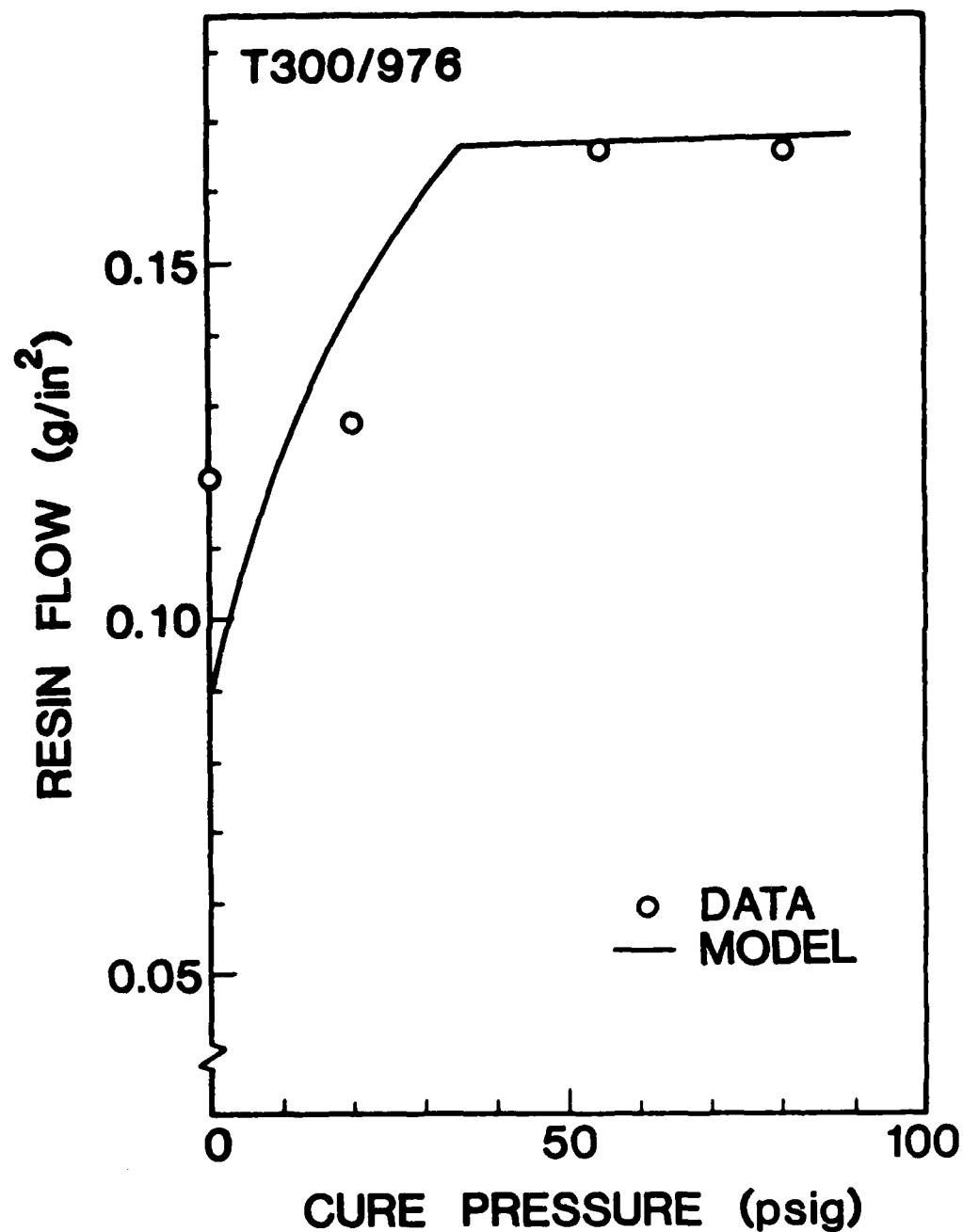


Fig. 12. Resin flow in Fiberite T300/976 unidirectional composites normal to the plies at the end of the cure. Comparisons between the data and the results computed by the Loos-Springer model [2]. Cure cycle given in Figure 11.

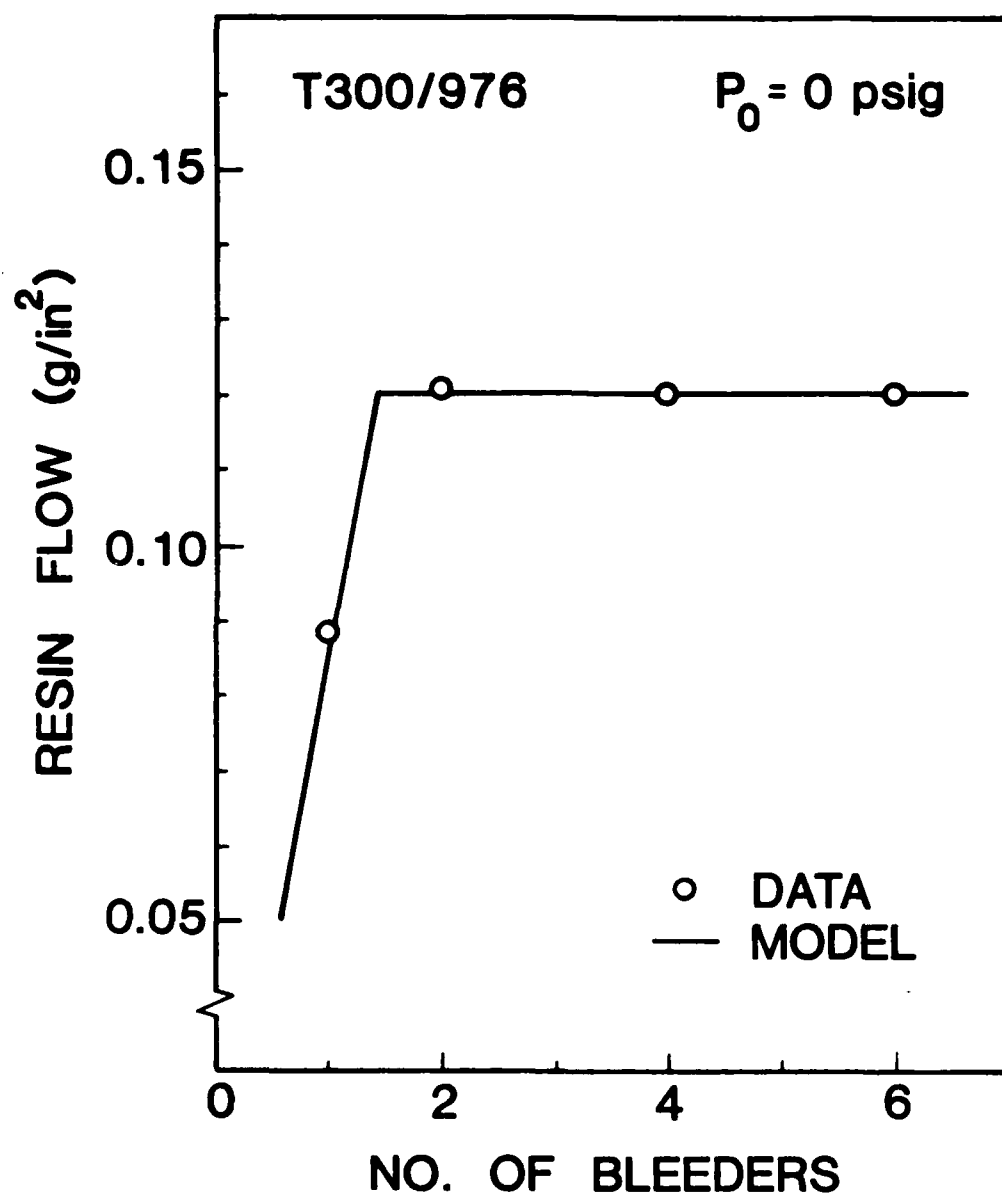


Fig. 13. Resin content in the bleeder for Fiberite T300/976 unidirectional composites at the end of the cure. Comparisons between the data and the results computed by the Loos-Springer model [2]. Cure cycle given in Figure 11.

TABLE 2**Properties of Hercules AS/3501-6 Prepreg**

Initial prepreg resin mass fraction	42 %
Initial thickness of prepreg	1.651×10^{-4} m
Resin content of one compacted ply	4.79×10^{-2} kg/m ²
Thickness of one compacted ply	1.194×10^{-4} m
Apparent permeability of the prepreg normal to the plane of the composite	5.8×10^{-16} m ²
Flow coefficient of the prepreg parallel to the fibers	1.7×10^2
Resin density	1.26×10^3 kg/m ³
Specific heat of the resin	1.26 kJ/kg/K
Thermal conductivity of the resin	1.67×10^{-1} W/m/K
Heat of reaction of the resin	See Ref. [10]
Fiber density	1.79×10^3 kg/m ³
Specific heat of the fiber	0.712 kJ/kg/K
Thermal conductivity of the fiber	26.0 W/m/K
Relationship between the cure rate, temperature, and degree of cure	See Ref. [12]
Relationship between the viscosity, temperature, and degree of cure	See Ref. [12]

TABLE 3**Properties of Fiberite T300/976 Prepreg**

Initial prepreg resin mass fraction	33 %
Initial thickness of prepreg	1.61×10^{-4} m
Resin content of one compacted ply	5.08×10^{-2} kg/m ²
Thickness of one compacted ply	1.35×10^{-4} m
Apparent permeability of the prepreg normal to the plane of the composite	2.4×10^{-17} m ²
Flow coefficient of the prepreg parallel to the fibers	1.7×10^2
Resin density	1.26×10^3 kg/m ³
Specific heat of the resin	1.26 kJ/kg/K
Thermal conductivity of the resin	1.67×10^{-1} W/m/K
Heat of reaction of the resin	See Ref.[3]
Fiber density	1.79×10^3 kg/m ³
Specific heat of the fiber	0.712 kJ/kg/K
Thermal conductivity of the fiber	26.0 W/m/K
Relationship between the cure rate, temperature, and degree of cure	See Ref.[3]
Relationship between the viscosity, temperature, and degree of cure	See Ref.[3]

Data relating the cure pressure to void content are presented below. First, however, an observation is made regarding the thickness of the bleeder.

When the bleeder is too thin, the bleeder will saturate before all the resin is removed from the laminate (Figures 13 and 14). It is important to note that the resin content of the laminate cannot be controlled by adjusting the bleeder thickness. While a thinner than necessary bleeder may result in the required "average" resin content, the resin in the laminate will be distributed nonuniformly (Figure 14). The reason for this is that resin is removed layer by layer as described previously (compaction process, Figure 3). Thus, unless the compaction process is complete, some of the layers will have the final (desired) resin content, while some will be resin rich.

Void Content

The effect of cure pressure on void content was examined by measuring the void contents of laminates cured at different pressures. In performing these tests no effort was made to minimize the void content, only to ensure reproducible data. The void contents of production laminates would generally be less than those of the laminates used in this study.

The void contents of eight-ply Fiberite T300/936 and T300/934 unidirectional laminates cured at different pressures were determined by examining optically the photomicrographs taken of compacted laminates after cure (Figure 15). The void contents thus measured are shown in Figure 16. In this figure, the void contents calculated by the Loos-Springer model is also included for the T300/976 laminates. The same calculations could not be performed for the T300/934 composite, because for this material the thermochemical data needed for the calculations were unavailable.

Three important observations can be made from the data in Figures 15 and 16. First, the void sizes do not vary appreciably across the laminate. Second, there was no apparent motion of the voids, implying that voids do not migrate through the resin. Third, there is reasonable agreement between the measured and predicted void content.

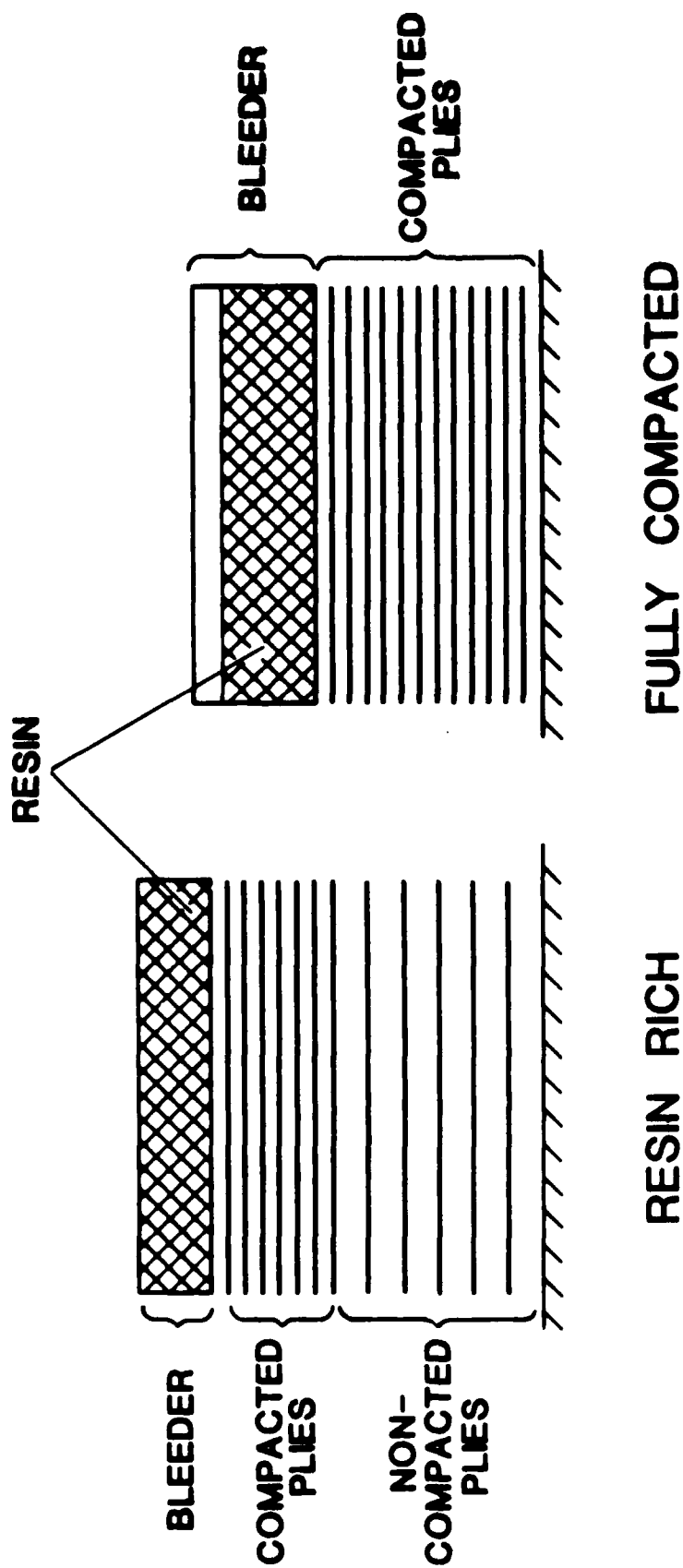


Fig. 14. Illustration of the effect of bleeder thickness. If the bleeder is too thin (left), the bleeder becomes saturated before compaction is complete and resin rich layers are present. For thick bleeder (right), all the resin is squeezed out at the end of the cure.

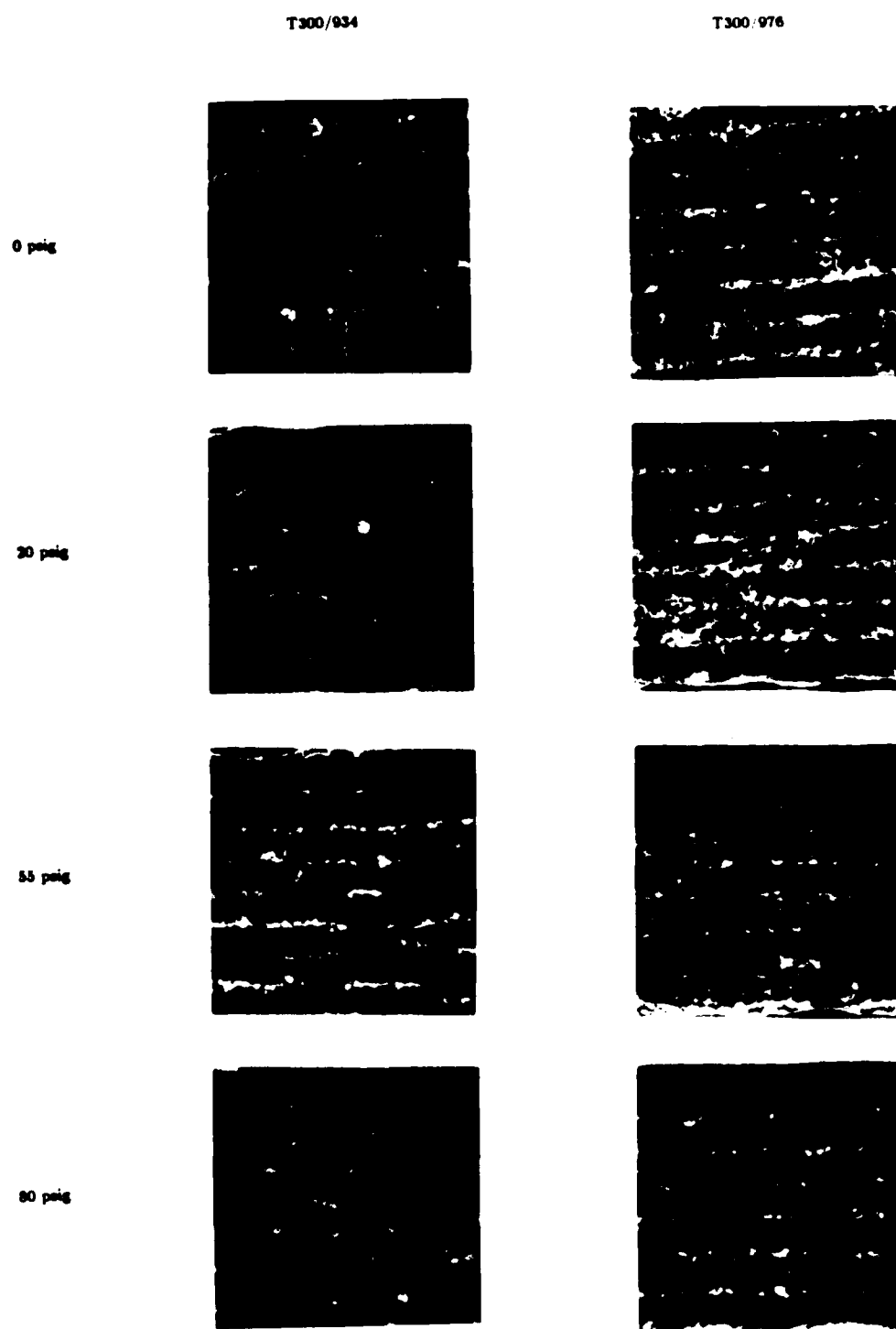


Fig. 15. Photomicrographs of eight ply Fiberite T300/976 and T300/934 laminates cured at 0 (vacuum bag), 20, 55, and 80 psig pressure. Magnification is 100 times. Temperature cure cycle is shown in Figure 11.

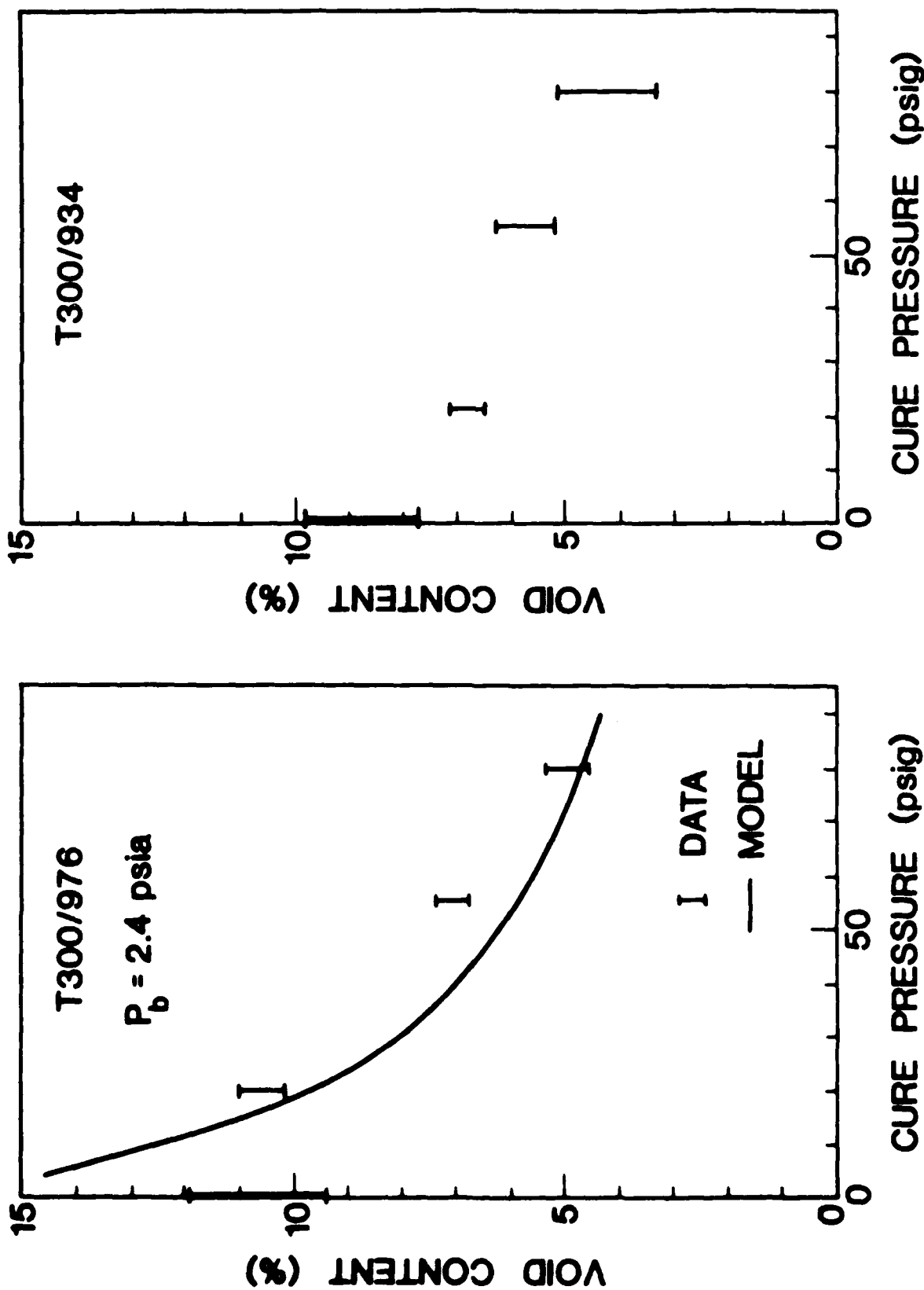


Fig. 16. Void contents as a function of cure pressure of Fiberite T300/976 and T300/934 eight-ply unidirectional laminates. Circles are data deduced from the photomicrographs of Figure 15. Bars represent spread in the data. Solid line is the result computed by the Loos-Springer model [2].

Section IV

MECHANICAL PROPERTIES

The cure pressure has a significant effect on the mechanical properties of composites. As was shown in the previous section the cure pressure influences the void content. In turn, the void content affects the mechanical properties. The compressive and interlaminar shear properties are especially affected by the cure pressure, since these properties are most sensitive to void content. For this reason, the compressive strengths and the short-beam shear strengths and moduli were measured as functions of cure pressure and void content.

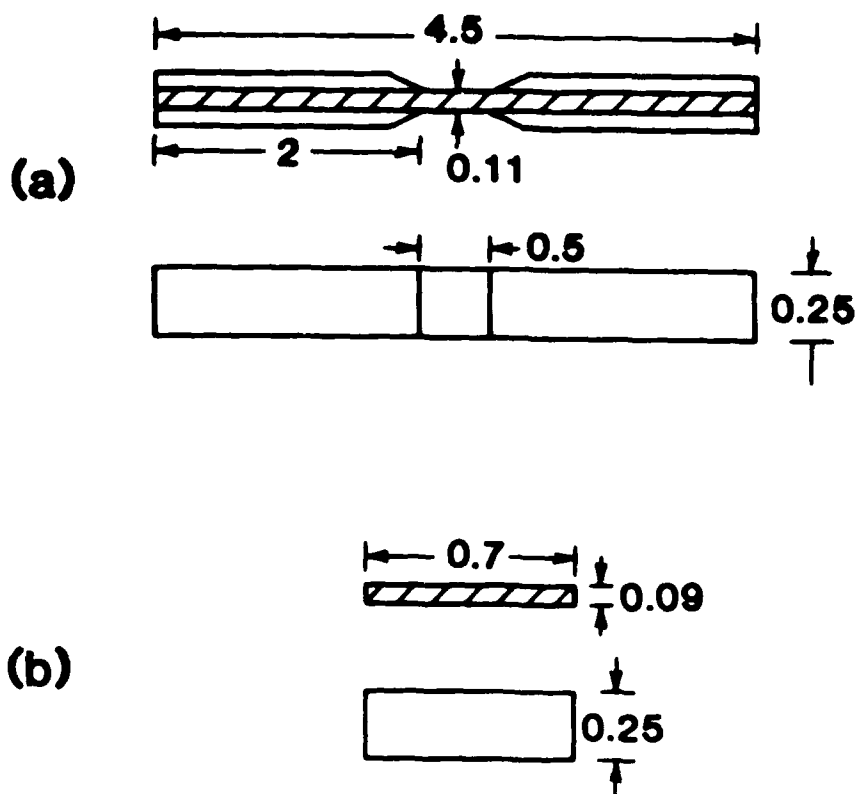
Unidirectional graphite-epoxy Fiberite T300/976 (16-ply) and T300/934 (20-ply) laminates were tested. The geometries of the specimens are shown in Figure 17. A Celanese fixture was used in the compression tests. The short-beam shear tests were performed according to the appropriate ASTM Standard [11]. The short-beam shear strengths and moduli were calculated by the expressions

$$\tau_s = \frac{0.75(P)}{(b)(h)} \quad (4)$$

$$E_s = \frac{(P)(s)^3}{4(d)(b)(h)^3} \quad (5)$$

where τ_s is the shear strength, E_s is the shear (flexure) modulus, P is the breaking load, b and h are width and thickness of specimen, respectively. d is the deflection at the center point, and s is the span between the supports.

The measured compressive and short-beam shear strengths and moduli are presented in Figures 18 and 19. Each point in these figures is the average of at least five data. These data show the effects of void content (and cure pressure) on these mechanical properties. As expected, both the strengths and the moduli increase with decreasing void content until the void content becomes about 3 to 4 percent. Below this void content neither the strengths nor the moduli change significantly. This suggests that it is not imperative to eliminate all the voids from the laminate. It is sufficient to keep the void content below a certain limit.



units in inches

Fig. 17. Geometries of the compression and short-beam shear specimens.

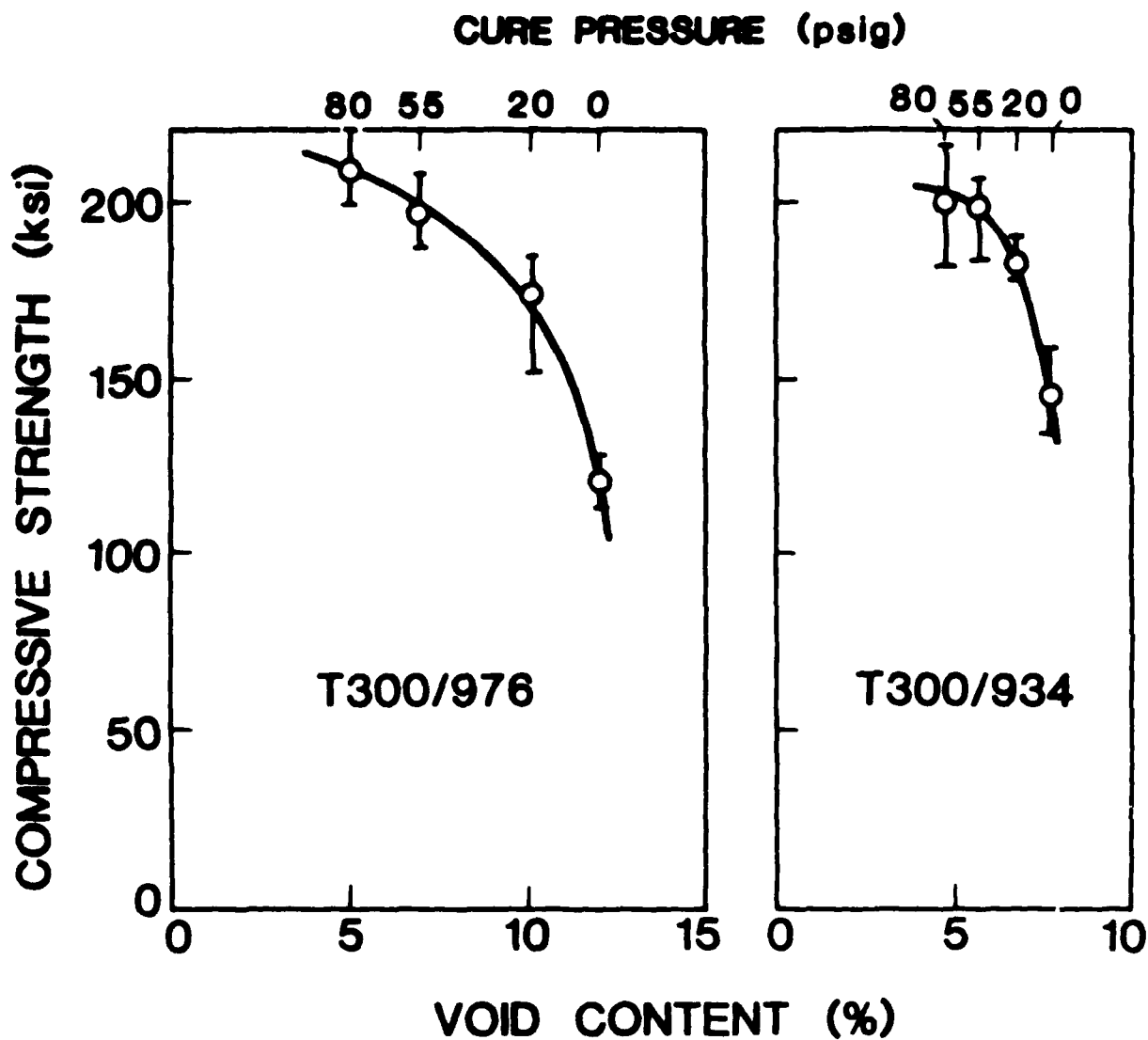


Fig. 18. The longitudinal compressive strengths of Fiberite T300/976 (16-ply) and T300/934 (20-ply) unidirectional laminates as a function of void content and cure pressure. Bars represent spread in the data. Cure cycle given in Figure 11.

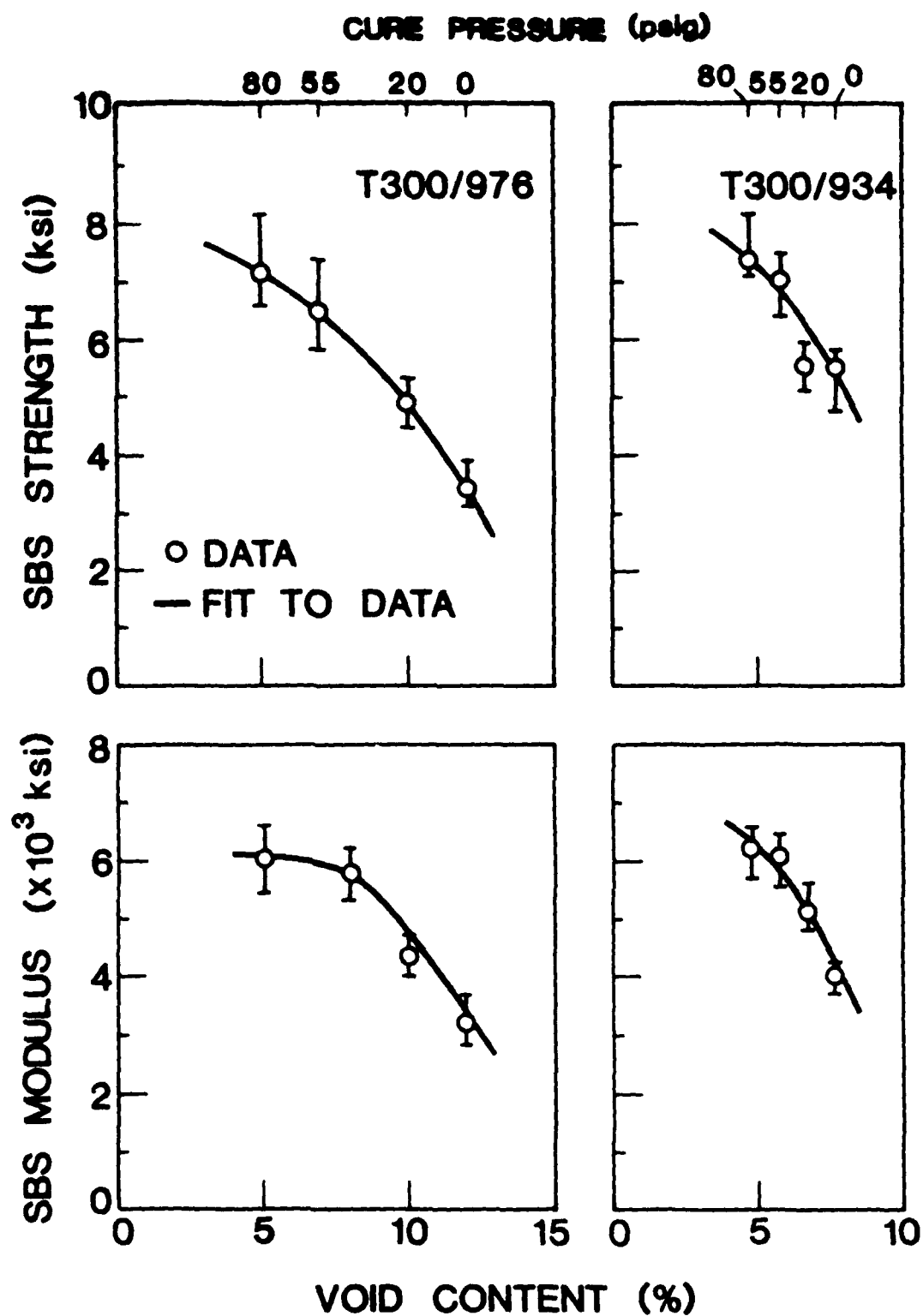


Fig. 19. The short-beam shear strengths and moduli of Fiberite T300/976 (16-ply) and T300/934 (20-ply) unidirectional laminates as a function of void content and cure pressure. Bars represent spread in the data. Cure cycle given in Figure 11.

Section V

CONCLUDING REMARKS

The experimental evidence presented in this technical report shows the important role the applied pressure plays in the cure process of fiber reinforced, thermoset resin composites. The pressure directly affects the compaction of the plies, the resin flow, and the void content and, indirectly (through the void content), the compressive and interlaminar shear properties.

Owing to its significance, the proper pressure must be applied during the cure. The appropriate cure pressure can best be established by models. One of the major objective of cure models is to predict the values of the following three parameters: a) compaction, b) resin flow, and c) void content. The exact knowledge of the pressure inside the laminate is not needed, as long as the pressure distribution included in the model predicts within acceptable accuracy the aforementioned three parameters.

The data also suggest that below a critical void content level, the void content does not significantly affect either the compressive or the interlaminar shear properties.

REFERENCES

1. Springer, G. S. "A Model of the Curing Process of Epoxy Matrix Composites," Progress in Science and Engineering of Composites, T. Hayashi, K. Kawata, and S. Umewaka, eds., Japan Society of Composite Materials, 1982, pp. 25-35.
2. Loos, A. C. and Springer, G. S. "Curing of Epoxy Matrix Composites," *Journal of Composite Materials*, Vol. 17 (1983), pp. 135-169.
3. Dusi, M. R., Lee, W. I., Ciriscioli, P. R. and Springer, G. S. "Cure Kinetics and Viscosity of Fiberite 976 Resin," *Journal of Composite Materials*, Vol. 21, 1987.
4. Campbell, F. C., Mallow, A. R., and Amuedo, K. C. "Computer Aided Curing of Composites," McDonnell-Douglas Corporation, St. Louis, Missouri, Report No. IR-0355-4, 1985.
5. Brand, R. A., Brown, G. G., and McKague, E. L. "Processing Science of Epoxy Resin Composites," Air Force Materials Laboratory Report, AFWAL-TR-83-4124, 1984.
6. Gutowski, T. G., Wineman, S. J., and Cai Z. "Applications of the Resin Flow/Fiber Deformation Model," in *Material Sciences for the Future*, Society for the Advancement of Materials and Process Engineering (SAMP) (1986), pp. 245-254.
7. Gutowski, T. G. "A Resin Flow/Fiber Deformation Model for Composites," in *Advancing Technology in Materials and Processes*, Society for the Advancement of Material and Process Engineering (SAMPE) (1985), pp. 925-934.
8. Gutowski, T. G., Morigaki, T., and Cai, Z. "The Consolidation of Laminate Composites," *Journal of Composite Materials*, (this issue).
9. Springer, G. S. "Resin Flow During the Cure of Fiber Reinforced Composites," *Journal of Composite Materials*, Vol. 16 (1982), pp. 400-410.
10. Loos, A. C. and Freeman, Jr., W. T. "Resin Flow During Autoclave Cure of Graphite-Epoxy Composites," *ASTM STP 873* (1985), pp. 119-130.
11. Standard Test Method for Apparent Interlaminar Shear Strength of Parallel Fiber Composites by Short-Beam Method, ANSI/ASTM Standard D2344-84 (1984).
12. Lee, W. I., Loos, A. C., and Springer, G. S., "Heat of Reaction, Degree of Cure, and Viscosity of Hercules 3501-6 Resin," *Journal of Composite Materials*, Vol. 16 (1982), pp. 510-520.

Appendix A

NUMBER OF COMPACTED PLIES

In time t the amount of resin flow per unit area normal to the plies is [2]

$$\dot{Q} = \frac{K}{\mu} \frac{\Delta P}{\Delta L} t \quad (\text{A-1})$$

where K is the permeability, and ΔP is the pressure drop across the distance ΔL . When resin flow is only in the direction normal to the plies the pressure drop can be approximated by

$$\Delta P \simeq P_o - P_b \quad (\text{A-2})$$

where P_o and P_b are the applied and bleeder pressures, respectively. The distance ΔL through which the pressure drop occurs is

$$\Delta L = n_c h_c + h_b \quad (\text{A-3})$$

where n_c is the number of compacted plies, h_c is the thickness of each compacted ply and h_b is the height of resin in the bleeder. The total amount of resin flow per unit area normal to the plies is

$$Q = n_c (h_o - h_c) \quad (\text{A-4})$$

where h_o is the thickness of each uncompactd ply. By combining Eqs. (A-1)–(A-4) we obtain

$$n_c = \sqrt{\frac{(K)(t)}{\mu (h_o - h_c) h_c} \frac{\sqrt{P_o - P_b}}{\sqrt{1 + \frac{h_b}{n_c h_c}}}} \quad (\text{A-5})$$

The number of compacted plies n_c is proportional to the resin depth in the bleeder h_b . Hence $h_b/(n_c h_c)$ is constant and Eq. (5) may be written as

$$n_c = C \sqrt{P_o - P_b} \quad (\text{A-6})$$

where C is a constant defined as

$$C = \sqrt{\frac{(K)(t)}{\mu (h_o - h_c) h_c} \frac{\sqrt{P_o - P_b}}{\sqrt{1 + \frac{h_b}{n_c h_c}}}} \quad (\text{A-7})$$

Appendix B

RESIN FLOW IN FIBERITE T300/934 LAMINATES

The resin flows in unidirectional Fiberite T300/934 laminates were also measured. These data were not included in the main text because thermochemical data for the 934 resin are lacking, preventing comparisons between the resin flow data and the model. Nevertheless, the resin flow data is included here (Figure B-1). It is hoped that these data will be useful to future investigators when thermochemical information on the Fiberite 934 resin becomes available.

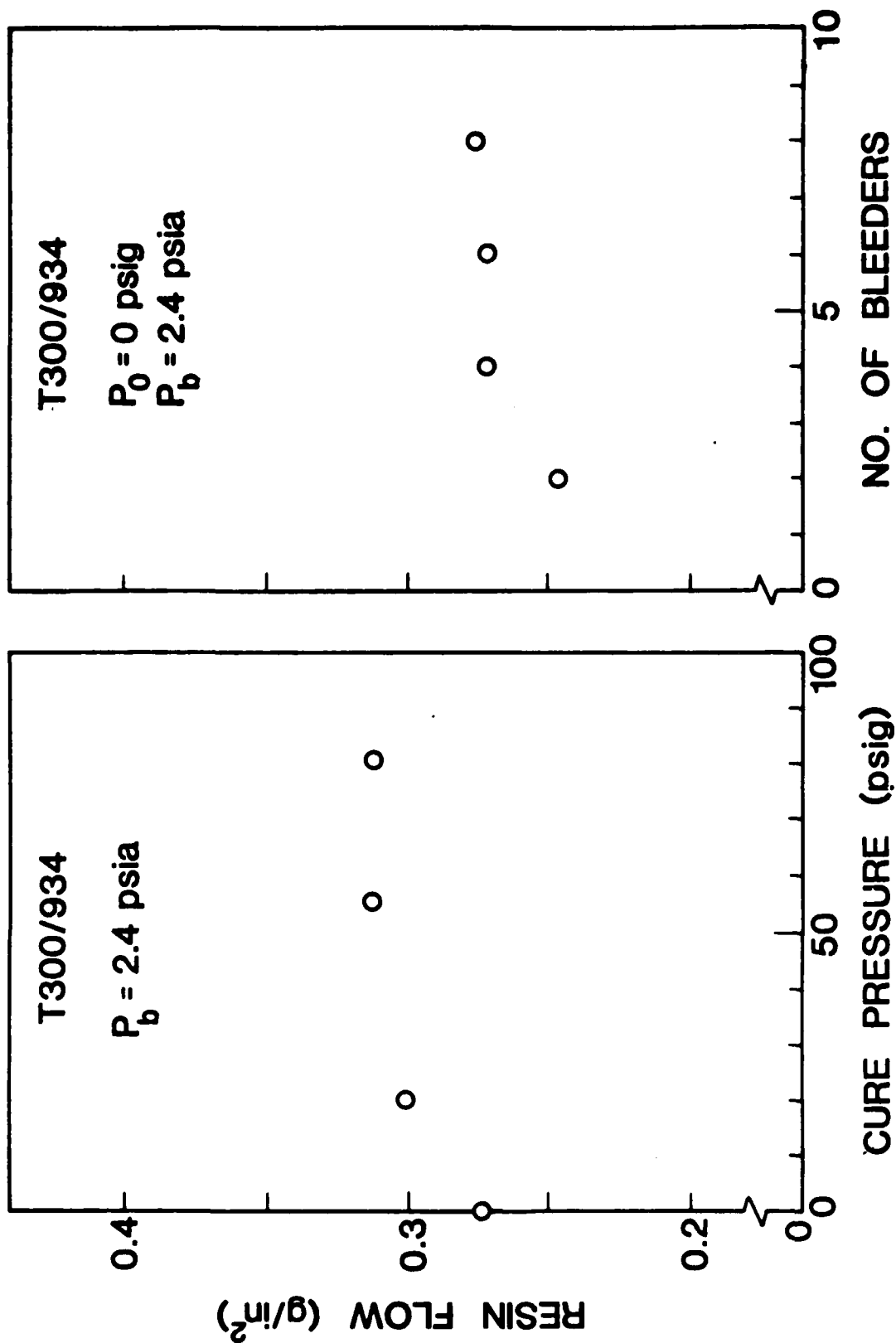


Fig. B-1. Resin flow in Fiberite T300/934 (20-ply) unidirectional composites normal to the plies as a function of cure pressure (left) and bleeder thickness (right) at the end of cure. Cure cycle given in Figure 11.

END

9-87

DTIC